2009

Nonlinear laser energy depletion in laser-plasma accelerators

Bradley Allan Shadwick
University of Nebraska-Lincoln, shadwick@unl.edu

Carl B. Schroeder
Lawrence Berkeley National Laboratory, Berkeley, California, cbschroeder@lbl.gov

Eric Esarey
Lawrence Berkeley National Laboratory, Berkeley, California, ehesarey@lbl.gov

Nonlinear laser energy depletion in laser-plasma accelerators[a)]

B. A. Shadwick,[1,b)] C. B. Schroeder,[2] and E. Esarey[2]
[1]*Department of Physics and Astronomy, University of Nebraska, Lincoln, Nebraska 68588-0111, USA*
[2]*Lawrence Berkeley National Laboratory, Berkeley, California 94720, USA*

(Received 7 December 2008; accepted 23 March 2009; published online 7 May 2009)

Energy depletion of intense, short-pulse lasers via excitation of plasma waves is investigated numerically and analytically. The evolution of a resonant laser pulse proceeds in two phases. In the first phase, the pulse steepens, compresses, and frequency redshifts as energy is deposited in the plasma. The second phase of evolution occurs after the pulse reaches a minimum length at which point the pulse rapidly lengthens, losing resonance with the plasma. Expressions for the rate of laser energy loss and rate of laser redshifting are derived and are found to be in excellent agreement with the direct numerical solution of the laser field evolution coupled to the plasma response. Both processes are shown to have the same characteristic length scale. In the high intensity limit, for nearly resonant Gaussian laser pulses, this scale length is shown to be independent of laser intensity. © *2009 American Institute of Physics*. [DOI: 10.1063/1.3124185]

I. INTRODUCTION

The evolution of a short, intense laser pulse propagating in an underdense plasma is of fundamental interest in plasma physics with application to fast ignition fusion, harmonic generation, x-ray lasers, and laser-plasma accelerators. Laser-plasma accelerators, for example, have demonstrated the production of high-quality electron bunches with energies up to 1 GeV using plasmas on the order of 1 cm.[1] A fundamental limit to the laser propagation distance, and consequently the single-stage energy gain in a laser-plasma accelerator, is the transfer of laser energy into plasma wave (wakefield) excitation.

In a laser wakefield accelerator,[2] an intense pulse with vector potential $A_\perp \sim mc^2/q$ will drive a large amplitude plasma wave with peak electric field $E_z \sim mc\omega_p/q$ when the laser pulse length satisfies the resonant condition $\omega_p L \sim 2c$, where $\omega_p = \sqrt{4\pi q^2 n_0/m}$ is the plasma frequency, n_0 is the ambient electron plasma density, q is the electron charge, m is the electron mass, and $L/\sqrt{2}$ is the rms pulse length of the laser vector potential. The loss of energy by the laser pulse, while propagating through plasma driving a wakefield, is generally referred to as pump depletion. The scale length over which the laser pulses depletes the bulk of its energy, L_{pd}, has been previously estimated by energy conservation arguments,[3,4] by equating the initial energy in the pulse to the energy left behind in the wake. Ting *et al.*[3] find $k_p L_{\mathrm{pd}} \simeq 4\pi k_0^2 k_p^{-2} a_0^{-2}$ for $a_0^2 \ll 1$, and $k_p L_{\mathrm{pd}} \simeq \sqrt{2}(k_0/k_p)^2 a_0/3$ for $a_0^2 \gg 1$, where $a_0 = qA_\perp^{\mathrm{peak}}/mc^2$ is the peak dimensionless vector potential and $k_p = \omega_p/c$ and $k_0 = \omega_0/c$ are the plasma and laser wavenumbers, respectively. Considering both the electrostatic and kinetic energies of the wake excited by a flattop laser pulse, Teychenné *et al.*[4] find $k_p L_{\mathrm{pd}} = 4k_0^2 k_p^{-2}\gamma_\perp^3(\gamma_\perp^2 - 1)E_2(1-\gamma_\perp^{-2})$, where $\gamma_\perp^2 = 1 + a_0^2/2$, and E_2 is the complete elliptic function of the second kind. Scale lengths for laser depletion have been derived in the weakly relativistic limit ($a_0 \ll 1$) for the plasma beat wave accelerator by Horton and Tajima[5] and for the standard laser wakefield accelerator by Bulanov *et al.*[6]

The energy gain by an electron bunch in a laser-driven plasma accelerator is determined by a number of factors that roughly reduce to the product of the electric field of the plasma wave and the effective acceleration length (laser-plasma interaction length). The longitudinal field of the laser-driven plasma wave is determined in large part by the dynamics of the laser pulse (though beam-loading effects also come into play). The effective acceleration length is also largely determined by the evolution of the laser pulse. For typical laser-plasma parameters, the most significant limitation on acceleration length is due to laser diffraction. Without some manner of optical guiding, the distance over which the electron bunch is subject to a significant accelerating gradient will be limited to a few Rayleigh ranges.

Extension of the laser-plasma interaction length to many Rayleigh ranges has been achieved through a combination of preformed plasma channel guiding, relativistic self-focusing, and ponderomotive self-channeling, enabling production of high-quality electron beam energies from 100 MeV (Refs. 7–10) to 1 GeV.[1,11,12] These guiding mechanisms can lead to near balance of transverse forces and little evolution of the spot size. As a result, the dynamics of the laser pulse are largely governed by longitudinal dynamics. For this reason we restrict our discussion to a one-dimensional plasma to fully understand the phenomenology associated with the longitudinal dynamics of the laser pulse. Results incorporating transverse dynamics will be the subject of a future paper.

Although various scaling laws have been derived previously based on energy balance arguments for specific pulse shapes, a detailed study of pump depletion for large laser intensities, including comparison to accurate numerical models, is lacking. We present a comprehensive numerical study of laser depletion via solutions to the Maxwell equations coupled to a fluid plasma response. In addition, we develop an analytical theory for the rate of change of the laser pulse

[a)]Paper DI2 3, Bull. Am. Phys. Soc. **53**, 77 (2008).
[b)]Invited speaker. Electronic mail: shadwick@mailaps.org.

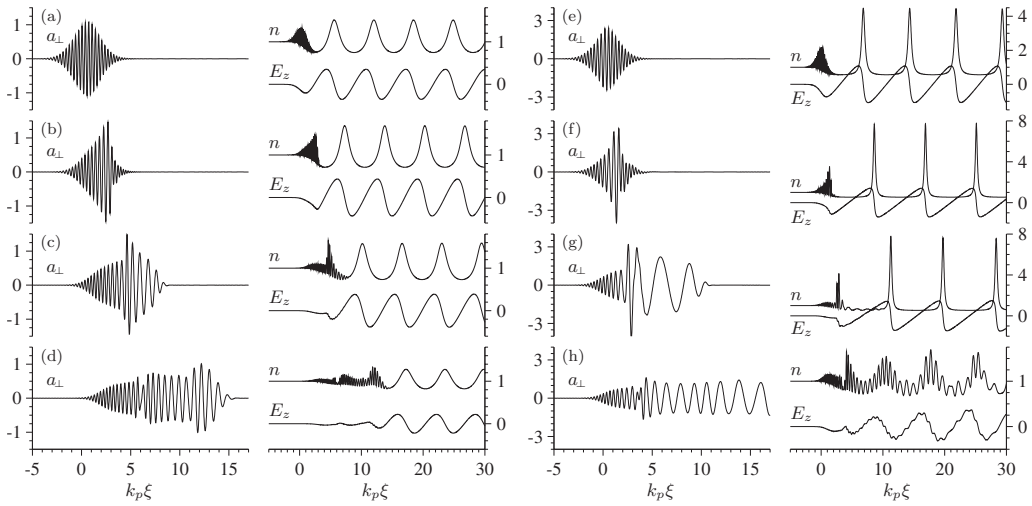

FIG. 1. Laser ($a_\perp$) evolution and cold fluid plasma response (n and E_z) for $k_0=20k_p$, $k_pL=2$, and $a_0=1$ [(a)–(d)] (right) and $a_0=2$ [(e)–(h)] (left). Time increases from top to bottom. For $a_0=1$: (a) $\omega_p t=500$; (b) $\omega_p t=1500$; (c) $\omega_p t=2500$; and (d) $\omega_p t=3500$. For $a_0=2$: (e) $\omega_p t=500$; (f) $\omega_p t=1000$; (g) $\omega_p t=1500$; and (h) $\omega_p t=2000$. The evolution in the two cases follows the same general pattern: pulse steepening due to self-phase modulation leading to an increase in wakefield amplitude followed by a dramatic increase in the length of the laser pulse and a corresponding decrease in wake amplitude. The longitudinal electric field E_z is shown as a multiple of $E_0=mc\omega_p/q$ while the plasma density n is shown as a multiple of the initial density n_0.

energy which is shown to be in excellent agreement with the numerical solutions.

II. LASER EVOLUTION

To study the laser evolution and plasma wave excitation, we solve the full one-dimensional fluid-Maxwell equations numerically. We cast the fluid equations for the plasma density n, and momentum $\boldsymbol{p}$, as well as Maxwell's equations for $\boldsymbol{E}$ and $\boldsymbol{B}$ in the comoving coordinates, $(t,\xi=ct-z)$:

$$\begin{aligned}
&\partial_t n+\partial_\xi[n(c-v_z)]=0,\\
&\partial_t p_x+(c-v_z)\partial_\xi p_x=q\left(E_x-\frac{v_z}{c}B_y\right),\\
&\partial_t p_z+(c-v_z)\partial_\xi p_z=q\left(E_z+\frac{v_x}{c}B_y\right),\\
&\partial_t E_x-c\partial_\xi B_y=-4\pi qnv_x,\\
&\partial_t E_z+c\partial_\xi B_y=-4\pi qnv_z,\\
&\partial_t B_y-c\partial_\xi E_x=0,
\end{aligned}\tag{1}$$

where $\boldsymbol{v}=\boldsymbol{p}/(m\gamma)$, $\gamma^2=1+p^2/(m^2c^2)$, and the plasma current is $\boldsymbol{j}=qn\boldsymbol{v}$. This system is conservative; in the moving window it is a straightforward calculation to show that the total energy is given by

$$H=\int_{\xi_1}^{\xi_2}d\xi\left(mc^2n\gamma+\frac{E^2+B^2}{8\pi}\right)+\int_0^t dt'[S^{(1)}-S^{(2)}],$$

where $S^{(1,2)}$ is the Poynting flux

$$S=mc^2n\gamma(c-v_z)+(c/8\pi)[E_z^2+(B_y-E_x)^2],$$

evaluated at the upstream (ξ_1) and downstream (ξ_2) coordinates of the window boundaries, respectively. At the upstream end, we assume no excitation precedes the laser, thus $S^{(1)}=mc^3n(\xi_1,t)$.

Figure 1 shows the laser evolution and plasma response for a near-resonant laser pulse as determined by Eq. (1) at selected times. Two case are shown: $a_0=1$ (left) resulting in a weakly nonlinear plasma wave; and $a_0=2$ (right) resulting in a strongly nonlinear plasma wave. In both cases $k_0=20k_p$ and the dimensionless vector potential is initially $qA_\perp/mc^2=a_\perp=a_0\exp(-\xi^2/L^2)\cos k_0\xi$. For the same parameters, Fig. 2 shows detailed evolution of: the laser pulse $a_\perp$ [(a) and (e)]; the wakefield E_z [(b) and (f)]; the laser power spectral density (PSD), $|\tilde{a}_\perp(k,t)|^2$, [(c) and (g)]; and the mean wavenumber $\langle k\rangle$ computed from the first moment of the laser PSD, the laser energy, and wave action [(d) and (h)].

The dynamical equations are solved numerically (in dimensionless form) using the method of lines, an explicit finite-difference, time-domain approach.[13] The ξ-derivatives are approximated using second-order backward finite differences, yielding a set of ordinary differential equations for each spatial grid point, which are advanced in time using a second-order Runge–Kutta method. No other approximations are involved in solving Eq. (1), in particular, the high-frequency oscillations of the laser are explicitly retained. All computations were preformed with $k_0\Delta\xi=1/32$ (approximately 200 gridpoints per laser wavelength) and $\omega_p\Delta t=k_p\Delta\xi/4$, which is dictated by stability requirements. As will be discussed below, this resolution was required to accurately capture the change in laser wavenumber as the pulse depleted. For the results presented, H varied by less than 1 in 10^4 over the entire calculation.

As the laser pulse propagates, its shape evolves due to interaction with the plasma. The plasma is modulated within the laser pulse which initially leads to a steepening of the laser pulse[6,14,15] due to frequency redshifting and the variation of local group velocity throughout the pulse: the trailing

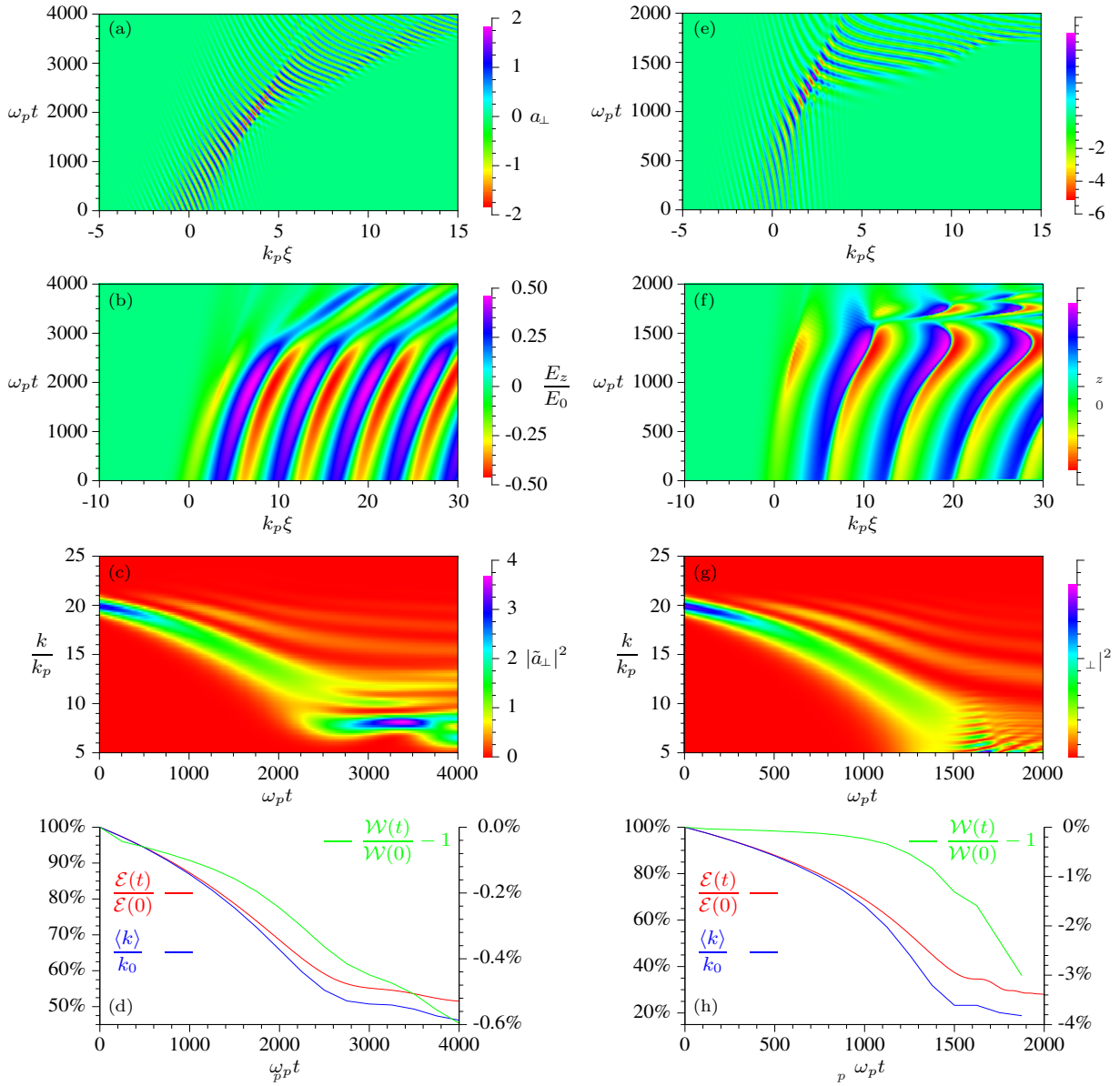

FIG. 2. (Color) Details of the system evolution for $k_0 = 20 k_p$, $k_p L = 2$, and $a_0 = 1$ [(a)–(d)] (right) and $a_0 = 2$ [(e)–(h)] (left). Shown is the evolution of the laser pulse [(a) and (e)]; the wakefield [(b) and (f)]; the laser vector potential PSD in arbitrary units [(c) and (g)]; laser energy $\mathcal{E}$ (red), the mean wavenumber $\langle k \rangle$ computed from the first moment of the laser vector potential PSD (blue), each normalized to their respective initial values (left axis), and the relative change in the wave action $\mathcal{W}$ (green; right axis) [(d) and (h)].

edge of the pulse sees a lower plasma density and consequently has a higher local group velocity than the leading edge. This results in a longitudinal compression of the pulse leading to a larger amplitude and to a non-Gaussian, skewed laser profile. The increased laser amplitude leads to both a larger wake amplitude and, consequently to a phase shift of the wakefield, as is evident in Fig. 2.

For the $a_0 = 1$ case, the pulse reaches its maximum amplitude at approximately $\omega_p t = 2000$. Consistent with this is the growth of the wakefield amplitude. The effects of laser frequency redshifting are also visible; the back of the laser pulse has a longer wavelength, as illustrated in Fig. 1. The gradient in density at the back of the laser pulse leads to a gradient in local laser phase velocity and, therefore, to growing separation of the peaks of the laser field and increasing wavelength. After $\omega_p t = 2000$, the pulse length begins to dramatically increase. At approximately $\omega_p t = 3000$, the pulse becomes sufficiently long to lose resonance with the plasma resulting in a much diminished wake amplitude. The laser energy [Fig. 2(d)] has an inflection point at approximately $\omega_p t = 2000$ corresponding to the time of largest laser amplitude. The knee in this curve near $\omega_p t = 2600$ points to the short time interval over which the pulse length expands. The reduction in slope at subsequent times is due to the loss of resonance, leading to weaker coupling and reduced transfer of laser energy to the plasma. Figure 2(c) shows the PSD, $|a_\perp(k)|^2$, of the laser pulse. Both redshifting due to depletion and the formation of sidebands (related to envelope distortions) are visible. The redshifting is proportional to the gradient in plasma density,[16] $\omega/\omega_p \simeq 1 - (\omega_p^2/2\omega_0^2) \int c dt \partial_\xi (n/n_0 \gamma)$, and therefore the redshifting is most pronounced at the back of the laser pulse, where the

plasma density gradient is large. Figure 2(c) also shows the evolution of the mean wavenumber $\langle k\rangle$ and the wave action $\mathcal{W}$ (see Sec. II C). As the pulse evolves, $\langle k\rangle$ closely tracks the energy evolution until the pulse distortion becomes significant. Throughout the entire evolution of the laser, the wave action, though only approximately invariant,[6,17] changes very little.

For $a_0=2$, the evolution of the system is qualitatively similar but more rapid, with the most striking difference being the rapid change in wakefield phase velocity (as inferred from the phase fronts) at $\omega_p t\approx 1400$; see Figs. 2(b) and 2(f).

A. Pulse energy evolution

The laser field will drive a transverse plasma current $4\pi j_\perp = 4\pi qnv_\perp = \omega_p^2(mc^2/q)(n/n_0)a_\perp/\gamma$, that will do work, extracting energy from the laser pulse. The wave equation for the laser in the comoving variables may be written as $(-2c\partial_{\xi t}^2-\partial_t^2)a_\perp=\omega_p^2\rho a_\perp$, where $\rho=(n/n_0)/\gamma$. We represent the laser field by a complex envelope $\hat{a}$ and central wavenumber k_0: $a_\perp=\mathrm{Re}[\hat{a}\exp(-ik_0\xi)]$, and assume $|\partial_{ct}\hat{a}|\ll|\partial_\xi\hat{a}|$. Furthermore, we will consider only propagation in an underdense plasma $k_p\ll k_0$ and assume a short laser pulse, $k_pL\sim 2$. With these assumptions, the wave equation becomes $(ik_0-\partial_\xi)\partial_{ct}\hat{a}=k_p^2\rho\hat{a}/2$, where we have neglected $\partial_{ct}^2\hat{a}$ and averaged ρ over the fast laser oscillation. Without further approximation, the laser wave equation can be expressed as

$$\partial_{ct}|(1+ik_0^{-1}\partial_\xi)\hat{a}|^2=-\frac{k_p^2}{2k_0^2}\rho\partial_\xi|\hat{a}|^2. \tag{2}$$

An evolution equation for the normalized laser energy, $\mathcal{E}=\int d(k_p\xi)|(1+ik_0^{-1}\partial_\xi)\hat{a}|^2$, is obtained by integrating Eq. (2),

$$\frac{\partial\mathcal{E}}{\partial\omega_p t}=-\frac{k_p^2}{2k_0^2}\int d\xi\rho\partial_\xi|\hat{a}|^2=\frac{k_p^2}{2k_0^2}\int d\xi|\hat{a}|^2\partial_\xi\rho. \tag{3}$$

Equation (3) describes the cost in laser energy for excitation of a plasma wave, and may be written as[6]

$$\frac{\partial}{\partial ct}\int d\xi(E_\perp^2+B_\perp^2)/8\pi=\frac{E_0^2}{16\pi}\int d\xi|\hat{a}|^2\partial_\xi\rho, \tag{4}$$

where $E_0=mc\omega_p/q$. For a short laser pulse, $\partial_\xi\rho<0$, and energy is extracted from the laser.

Assuming a quasistatic plasma response, the integral in Eq. (3) may be evaluated as follows. In the quasistatic approximation,[18] the dimensionless electrostatic potential ϕ satisfies

$$\frac{\partial^2\phi}{\partial(k_p\xi)^2}=\frac{1}{2}\left[\frac{\gamma_\perp^2}{(1+\phi)^2}-1\right], \tag{5}$$

where $\gamma_\perp^2=1+|\hat{a}|^2/2$ is the Lorentz factor associated with the electron quiver motion and $\rho=(1+\phi)^{-1}$. Solving Eq. (5) for $|\hat{a}|^2$, we have

$$|\hat{a}|^2\partial_\xi(1+\phi)^{-1}=-2\partial_\xi[1+\phi+(1+\phi)^{-1}+(\partial_{k_p\xi}\phi)^2].$$

Therefore, the energy evolution equation (3) can be written as $\partial_{\omega_p t}\mathcal{E}=$const. The constant can be evaluated from the first integral of Eq. (5). Before the laser, ϕ and $\partial_\xi\phi$ are identically zero. Behind the laser pulse ($\gamma_\perp=1$), the first integral of Eq. (5) is

$$(\partial\phi/\partial k_p\xi)^2=(E_{\max}/E_0)^2+1-\phi-(1+\phi)^{-1}, \tag{6}$$

where $E_{\max}$ is the maximum electric field amplitude behind the laser. Therefore the evolution equation for the laser energy is

$$\partial\mathcal{E}/\partial\omega_p t=-(k_p^2/k_0^2)(E_{\max}/E_0)^2. \tag{7}$$

For a quasistatic plasma response, the gradient in laser energy is determined by the amplitude of the laser-driven plasma wave field. This is a general result, independent of laser pulse shape or intensity.

For a flattop laser pulse of optimally matched pulse length,[18,19] $E_{\max}/E_0=(\gamma_\perp^2-1)/\gamma_\perp$, and the energy evolves as $\partial\mathcal{E}/\partial\omega_p t=-(k_p^2/k_0^2)(\gamma_\perp^2-1)^2/\gamma_\perp^2$. In the weakly relativistic regime $|\hat{a}|\ll 1$, $\partial_t\mathcal{E}\propto-|\hat{a}|^4$, and, for ultraintense laser pulses $|\hat{a}|\gg 1$, $\partial_t\mathcal{E}\propto-|\hat{a}|^2$.

Figure 3 shows the laser energy evolution versus normalized distance k_p^3z/k_0^2 for a range of laser intensities and ratios of the laser and plasma frequency. (All results shown in Fig. 3 and subsequent figures take the initial laser pulse profile to be a Gaussian with $k_pL=2$.) At early times, we see the (k_p^3z/k_0^2)-dependence in the energy evolution. The emergence of additional k-dependence at later times ($k_pz\gtrsim\pi k_p^2/k_0^2$) is not an indication that the quasistatic plasma response for wake excitation is no longer valid, but rather that the laser evolution contains additional k-dependence in the nonparaxial operator of Eq. (2) and the neglected operator $\partial_{ct}^2\hat{a}$.

Figure 4 shows the amplitude of the field of the excited plasma wave $E_{\max}/E_0$. Self-steepening of the laser pulse increases the laser intensity and the amplitude of the plasma wave. This is the source of the increasing rate of energy

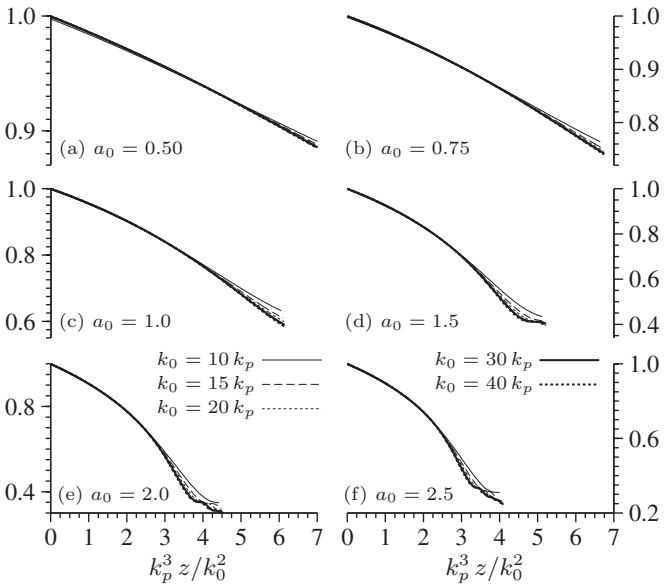

FIG. 3. Laser pulse energy, normalized to the initial value, for various initial laser intensities and wavenumbers.

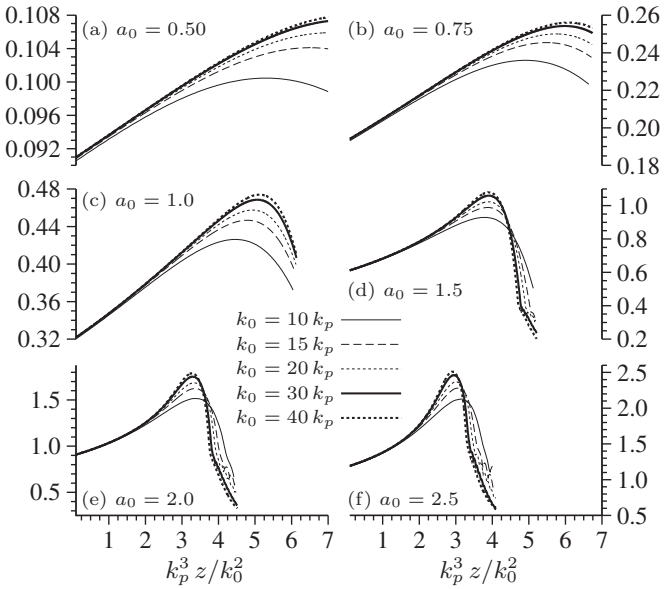

FIG. 4. Evolution of the maximum wakefield amplitude, E_{max}/E_0, for various initial laser intensities and wavenumbers.

deposition observed in Fig. 3, i.e., the departure from a linear decrease in laser energy. Shown in Fig. 5 is a comparison of the rate of change in the laser energy (solid lines) compared to the prediction of Eq. (7) (symbols), with E_{max}/E_0 as shown in Fig. 4. Overall the agreement is excellent. This is due to the fact that Eq. (7) is an instantaneous expression for the rate of energy loss; the neglected term in the wave equation evidently remain small and, at any instant in time, the quasistatic plasma remains a very good approximation.

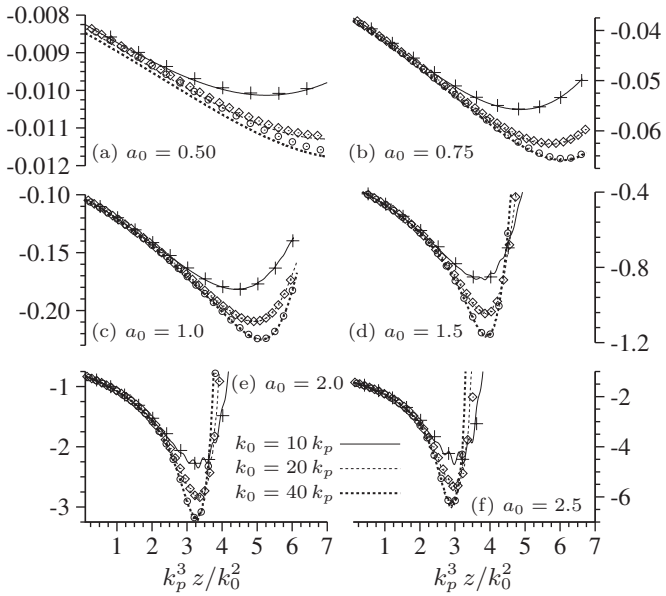

FIG. 5. Rate of change in laser energy, $\partial\mathcal{E}/\partial\omega_p t$, (lines), compared to Eq. (7) (symbols: $k_0=10k_p$, crosses; $k_0=20k_p$, diamonds; and $k_0=40k_p$ circles), for various initial laser intensities and wavenumbers.

B. Pump depletion length

The characteristic scale length of laser energy deposition into plasma wave excitation, i.e., pump depletion length, L_{pd} may be defined as

$$\partial\mathcal{E}/\partial_{ct} \equiv -\mathcal{E}/L_{pd}, \tag{8}$$

or $k_pL_{pd}=(k_0/k_p)^2(E_0/E_{max})^2\mathcal{E}$. The pump depletion length may also be written as $L_{pd}E_{max}^2=\int d\xi(E_\perp^2+B_\perp^2)$.

For a flattop laser pulse of optimal length [i.e., for laser pulse length of $k_pL_{opt}=2\gamma_\perp E_2(1-\gamma_\perp^{-2})$, where E_2 is the complete elliptic integral of the second kind[18,19]], the initial pump depletion length can be evaluated,

$$k_pL_{pd} = \frac{k_0^2}{k_p^2}\frac{2\gamma_\perp^2 k_pL_{opt}}{\gamma_\perp^2-1} \approx \frac{k_0^2}{k_p^2}\begin{cases} 4\pi/a_0^2 & \text{for } a_0^2 \ll 1, \\ 2^{3/2}a_0 & \text{for } a_0^2 \gg 1, \end{cases} \tag{9}$$

where $E_{max}=(\gamma_\perp^2-1)/\gamma_\perp$ and $\mathcal{E}\simeq L_{opt}a_0^2=2L_{opt}(\gamma_\perp^2-1)$ to leading order. The minimum pump depletion length occurs at $a_0\approx 2.3$. Equation (9) was obtained in Ref. 4 based on energy conservation arguments. Although the flattop pulse is simple to evaluate analytically, it is somewhat unphysical as it is difficult to produce experimentally. In addition, a flattop pulse has the property that the optimal pulse length increases with increasing a_0. In particular $k_pL_{opt}\simeq\sqrt{2}a_0$ for $a_0\gg 1$. This scaling is responsible for the linear scaling $L_{pd}\propto a_0$ at $a_0\gg 1$ in Eq. (9). In contrast, for a Gaussian pulse the optimal pulse length is approximately independent of a_0.

In general, the excitation of the plasma wave has a broad resonance. For a Gaussian of fixed pulse duration near linear resonance, solutions to Eq. (5) indicate that the plasma wave amplitude can be approximated as $E_{max}\simeq(\pi/2e)^{1/2}(\gamma_\perp^2-1)/\gamma_\perp$. Fixing the Gaussian pulse length at the linearly resonant value, the pump depletion length becomes

$$k_pL_{pd} \simeq \frac{k_0^2}{k_p^2}\frac{2^{5/2}e}{\pi^{1/2}}\frac{\gamma_\perp^2}{\gamma_\perp^2-1} \approx 8.7\frac{k_0^2}{k_p^2}\begin{cases} 2a_0^{-2}, & a_0^2 \ll 1, \\ 1, & a_0^2 \gg 1. \end{cases} \tag{10}$$

In this case, the pump depletion length is independent of laser intensity for $a_0\gg 1$.

If we assume an initially linear increase in wake amplitude with scale length equal to the depletion length, $E_{max}(z)/E_{max}(0)\simeq 1+z/L_{pd}$, as results from the steepening of $a_\perp^2$ and as indicated in Fig. 4 for $z\ll L_{pd}$, then Eq. (7) predicts the length to deplete a fraction of the laser energy $\Delta\mathcal{E}=1-\mathcal{E}/\mathcal{E}(0)$ is $\hat{L}_{pd}=L_{pd}^{(0)}(\Delta\mathcal{E}-\Delta\mathcal{E}^2)$, where $L_{pd}^{(0)}$ is the pump depletion length at $z=0$.

Figure 6 shows the length to deplete a fraction of the laser energy versus laser intensity. The gray curves are $\hat{L}_{pd}$ with $L_{pd}^{(0)}$ given by Eq. (10) for a resonant Gaussian laser pulse. Agreement is excellent for $\Delta\mathcal{E}\ll 1$ (i.e., for $z\ll L_{pd}^{(0)}$). Departure from the analytic pump depletion length occurs deep into depletion due to laser pulse deformation; laser profile changes result in a larger wake excitation and increased energy deposition. Hence, in deep depletion, the analytic pump depletion length will overestimate the length required to deposit a fraction of the laser energy (as shown in Fig. 6).

The depletion scale length defined in Eq. (8) can also be derived heuristically.[3,4] Consider the length for which the total field energy in the plasma wave is equal to half the

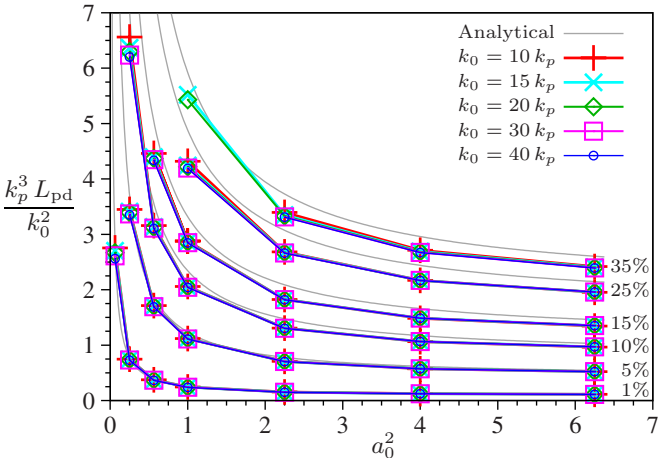

FIG. 6. (Color online) Pump depletion lengths for selected fractional energy loss and various values of k_0 from direct solution of Eq. (1) (symbols) and $\hat{L}_{\rm pd}$ with $\hat{L}_{\rm pd}^{(0)}$ given by Eq. (10) for a resonant Gaussian laser pulse (gray line, no symbols).

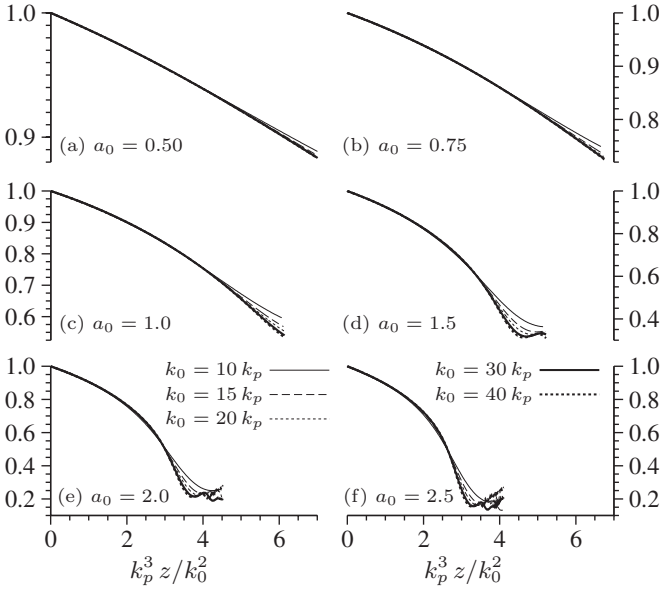

FIG. 7. Mean laser wavenumber, normalized to k_0 vs propagation distance $k_p^3 z/k_0^2$, for various laser intensities.

initial laser energy. That is, approximating the total plasma wave energy density (averaged over many oscillations) as $E_{\rm max}^2/16\pi$ and setting $L_{\rm pd}(E_{\rm max}^2/16\pi) \sim k_p^{-1}(mc\omega_0/e)^2\mathcal{E}/16\pi$, yields $L_{\rm pd} \sim (k_0^2/k_p^3)(E_0/E_{\rm max})^2\mathcal{E}$.

C. Laser redshifting

The mean wavenumber of the pulse, $\langle k\rangle$, may be defined as the first moment of the vector potential PSD,

$$\langle k\rangle = \int_0^\infty dk k|\tilde{a}_\perp(k)|^2 \Big/ \int_0^\infty dk|\tilde{a}_\perp(k)|^2, \tag{11}$$

where $\tilde{a}_\perp(k)$ is the Fourier transform in ξ of $a_\perp$. Using standard Fourier transform relations, it can be shown that

$$\int_0^\infty dk k|\tilde{a}_\perp(k)|^2 = -\int_{-\infty}^\infty d\xi H[a_\perp](\xi)\partial_\xi a_\perp,$$

where $H[a_\perp]$ is the Hilbert transform of $a_\perp$. Expressing $a_\perp$ in terms of the envelope $\hat{a}$ and averaging over the fast time scale, we find $-\int_{-\infty}^\infty d\xi H[a_\perp](\xi)\partial_\xi a_\perp = \frac{1}{2}\int d\xi[k_0|\hat{a}|^2 + \mathrm{Im}(\hat{a}^*\partial_\xi\hat{a})] = \frac{1}{2}\mathcal{W}$, where $\mathcal{W}$ is the wave action. Thus we have $\langle k\rangle = \frac{1}{2}\mathcal{W}/\int_0^\infty dk|\tilde{a}_\perp(k)|^2$. In terms of $a_\perp$, the normalized pulse energy is $k_0^2\mathcal{E} = \int d(k_p\xi)(\partial_\xi a_\perp)^2 = 2k_p\int_0^\infty dk k^2|\tilde{a}_\perp|^2$. At early time, before the pulse envelope has distorted significantly, we can approximate this as $k_0^2\mathcal{E} \approx 2\langle k\rangle^2 k_p\int_0^\infty dk|\tilde{a}_\perp(k)|^2$ and we have $\langle k\rangle = k_0^2\mathcal{E}/(k_p\mathcal{W})$. The disparity between the laser and plasma time scales, leads to the adiabatic invariance of the wave action[6,17] and thus

$$\langle k\rangle^{-1}\partial_{ct}\langle k\rangle = \mathcal{E}^{-1}\partial_{ct}\mathcal{E} = -1/L_{\rm pd}. \tag{12}$$

Hence the central laser wavenumber redshifts $\partial_t\langle k\rangle < 0$ with the characteristic scale length equal to $L_{\rm pd}$. Figure 7 shows the evolution of the mean laser wavenumber versus $k_p^3 z/k_0^2$. Comparison between Figs. 7 and 3 shows excellent agreement with Eq. (12).

Numerically, accurately capturing small changes in $\langle k\rangle$ requires particularly fine resolution. To detect a shift of in wavenumber δk over N cycles in a quantity represented on a grid, requires a resolution that scales like $k_0\Delta\xi < 2N\pi\delta k/k_0$, suggesting that the resolution requirements scale like $(k_0/k_p)^2$. As can be seen in Fig. 5, $\partial_t\mathcal{E}$ is most accurate for moderate to large a_0 and for small k_0. Since all numerical results were obtained with constant $k_0\Delta\xi = 1/32$, we expect the cases where the relative wavenumber shifts are largest to yield the most accurate evolution of the laser energy, which is for moderate a_0 and small k_0.

D. Laser pulse length evolution

The evolution of the pulse length is shown in Fig. 8 for various values of normalized laser intensity a_0 and wavenumber ratio k_0/k_p. The laser pulse profile is initially Gaussian with length $k_pL = 2$. The pulse length is computed from

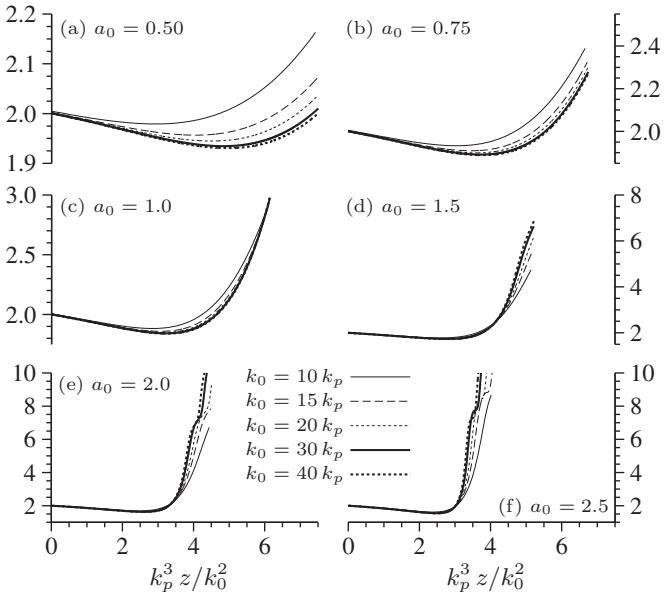

FIG. 8. Pulse length, k_pL, computed from the ξ-variance of the energy density, vs propagation distance $k_p^3 z/k_0^2$ for various laser intensities.

the ξ-variance of the energy density. Note that, as shown in Fig. 1, the pulse does not remain Gaussian, and the pulse will develop a significant third-order moment (skew). The laser pulse length exhibits some modest pulse compression, due to the wake-induced gradient in the index of refraction at the back of the pulse, followed by rapid expansion of the pulse (most pronounced in the $a_0 > 1$ cases).

III. CONCLUSION

Through a comprehensive numerical study, we have obtained a detailed description of energy depletion of intense, short-pulse lasers via resonant excitation of plasma waves in 1D. The rate of energy deposition into the plasma by the laser is a nonlinear process dependent on the laser pulse amplitude and length and the ratio of the plasma density to the critical density. Correspondingly, the pump depletion length depends on these same parameters in a complex way. The evolution of a resonant laser pulse proceeds in two phases. In the first phase, the pulse envelope is modified via self-phase modulation, resulting in pulse steepening and pulse compression. The central wavenumber of the pulse is reduced as energy is deposited in the plasma (redshifting). The second phase of evolution occurs after the pulse reaches a minimum length, at which point the pulse length rapidly lengthens, losing resonance with the plasma. This causes the plasma wave amplitude, and hence rate of laser energy depletion, to rapidly decrease.

An analytical theory was developed to describe the depletion process based on the 1D wave equation for the laser pulse coupled to the nonlinear quasistatic fluid equations. In particular, both the pulse energy and average wavenumber have the same intrinsic scale length: $\partial_{ct}\mathcal{E} = -\mathcal{E}/L_{\mathrm{pd}}$ and $\partial_{ct}\langle k\rangle = -\langle k\rangle/L_{\mathrm{pd}}$, where $k_p L_{\mathrm{pd}} = (k_0/k_p)^2 (E_0/E_{\max})^2 \mathcal{E}$. This result is general: it is fully nonlinear and valid for arbitrary pulse shape. This expression is found be to in excellent agreement with direct numerical solution of the unapproximated Maxwell-cold fluid equations over the entire propagation distance. This agreement suggests that at any instant in time, the quasistatic approximation to the plasma response is accurate for near-resonant laser pulses. Numerical modeling of laser depletion requires accurately resolving the laser frequency shifts, and hence a grid sufficiently small to resolve a small fraction of the laser wavelength.

This analysis was also used to derive analytical expressions for the pump depletion length. For an optimized flattop pulse, the pump depletion length is $k_p L_{\mathrm{pd}} \simeq (k_0^2/k_p^2)(4\pi/a_0^2)$ for $a_0^2 \ll 1$, and $k_p L_{\mathrm{pd}} \simeq (k_0^2/k_p^2)\sqrt{8}a_0$ for $a_0^2 \gg 1$, in agreement with previous estimates.[4,20] The numerical studies presented in this work took the initial laser pulse to have a linearly resonant Gaussian profile. Solutions of the quasistatic wakefield equation [Eq. (5)] indicate that, for a Gaussian laser profile, the wake amplitude is rather insensitive to the pulse length and that the pulse length corresponding to maximum wake amplitude is approximately the linearly resonant pulse length ($k_p L = 2$) over the laser intensity range of interest. For a linearly resonant Gaussian pulse, the depletion length was found to be $k_p L_{\mathrm{pd}} \simeq 17.4(k_0^2/k_p^2)/a_0^2$ for $a_0^2 \ll 1$, and $k_p L_{\mathrm{pd}} \simeq 8.7 k_0^2/k_p^2$ for $a_0^2 \gg 1$. Notice that in the high intensity limit, the depletion length is independent of intensity. These expressions for L_{pd} were found to be in good agreement with the numerical solutions of the full Maxwell-fluid equations for moderate laser depletion. For example, the length required to deplete 5% of the laser energy is $L_{\mathrm{pd}}/20$, the length required for 10% is $L_{\mathrm{pd}}/10$, etc. For deep depletion, the simple expressions for the depletion length underestimate the amount of energy loss. This is because pulse deformation results in increased wake amplitude and enhanced depletion. Numerical solutions indicate that significant depletion is possible ($\sim$50%) for $a_0 \sim 1-2$ before pulse lengthening causes loss of resonance with the plasma and reduction in the plasma wave amplitude.

Here we have assumed that the dynamics of laser depletion in a plasma channel can be adequately approximated by the longitudinal dynamics. A preliminary study in multidimensions indicates that this is a good approximation for matched pulses propagating in broad channels with a characteristic transverse dimension $r_0 \gg k_p^{-1}$. For such a matched pulse in a channel, pulse diffraction is balanced by channel focusing and self-focusing effects, resulting in minimal transverse evolution of the pulse. Furthermore it was assumed that the wakefield has not undergone complete cavitation of the plasma electrons, which is valid for intensities such that $a^2/\gamma_\perp < (k_p r_0)^2/2$. Nonlinear pulse evolution in multidimensions will be a topic of further study.

ACKNOWLEDGMENTS

Work at the UNL was supported by the U.S. Department of Energy under Contract No. DE-FG02-08ER55000. Work at the LBNL was supported by the Director, Office of Science, Office of High Energy Physics, of the U.S. Department of Energy under Contract No. DE-AC02-05CH11231.

[1] W. P. Leemans, B. Nagler, A. J. Gonsalves, Cs. Tóth, K. Nakamura, C. G. R. Geddes, E. Esarey, C. B. Schroeder, and S. M. Hooker, Nat. Phys. **2**, 696 (2006).
[2] E. Esarey, P. Sprangle, J. Krall, and A. Ting, IEEE Trans. Plasma Sci. **24**, 252 (1996).
[3] A. Ting, E. Esarey, and P. Sprangle, Phys. Fluids B **2**, 1390 (1990).
[4] D. Teychenné, G. Bonnaud, and J.-L. Bobin, Phys. Plasmas **1**, 1771 (1994).
[5] W. Horton and T. Tajima, Phys. Rev. A **34**, 4110 (1986).
[6] S. V. Bulanov, I. N. Inovenkov, V. I. Kirsanov, N. M. Naumova, and A. S. Sakharov, Phys. Fluids B **4**, 1935 (1992).
[7] C. G. R. Geddes, C. Toth, J. van Tilborg, E. Esarey, C. B. Schroeder, D. Bruhwiler, C. Nieter, J. Cary, and W. P. Leemans, Nature (London) **431**, 538 (2004).
[8] S. P. D. Mangles, C. D. Murphy, Z. Najmudin, A. G. R. Thomas, J. L. Collier, A. E. Dangor, E. J. Divall, P. S. Foster, J. G. Gallacher, C. J. Hooker, D. A. Jaroszynski, A. J. Langley, W. B. Mori, P. A. Norreys, F. S. Tsung, R. Viskup, B. R. Walton, and K. Krushelnick, Nature (London) **431**, 535 (2004).
[9] J. Faure, Y. Glinec, A. Pukhov, S. Kiselev, S. Gordienko, E. Lefebvre, J. P. Rousseau, F. Burgy, and V. Malka, Nature (London) **431**, 541 (2004).
[10] T. P. Rowlands-Rees, C. Kamperidis, S. Kneip, A. J. Gonsalves, S. P. D. Mangles, J. G. Gallacher, E. Brunetti, T. Ibbotson, C. D. Murphy, P. S. Foster, M. J. V. Streeter, F. Budde, P. A. Norreys, D. A. Jaroszynski, K. Krushelnick, Z. Najmudin, and S. M. Hooker, Phys. Rev. Lett. **100**, 105005 (2008).
[11] K. Nakamura, B. Nagler, C. Toth, C. G. R. Geddes, C. B. Schroeder, E. Esarey, W. P. Leemans, A. J. Gonsalves, and S. M. Hooker, Phys. Plasmas **14**, 8 (2007).

[12]S. Karsch, J. Osterhoff, A. Popp, T. P. Rowlands-Rees, Zs. Major, M. Fuchs, B. Marx, R. Hörlein, K. Schmid, L. Veisz, S. Becker, U. Schramm, B. Hidding, G. Pretzler, D. Habs, F. Grüner, F. Krausz, and S. M. Hooker, New J. Phys. **9**, 415 (2007).
[13]The code used in these calculations is freely available for noncommercial purposes. Contact the author for details.
[14]D. F. Gordon, B. Hafizi, R. F. Hubbard, J. R. Peñano, P. Sprangle, and A. Ting, Phys. Rev. Lett. **90**, 215001 (2003).
[15]E. Esarey, C. B. Schroeder, B. A. Shadwick, J. S. Wurtele, and W. P. Leemans, Phys. Rev. Lett. **84**, 3081 (2000).
[16]E. Esarey, A. Ting, and P. Sprangle, Phys. Rev. A **42**, 3526 (1990).
[17]A. J. Brizard, Phys. Plasmas **5**, 1110 (1998).
[18]P. Sprangle, E. Esarey, and A. Ting, Phys. Rev. Lett. **64**, 2011 (1990).
[19]V. I. Berezhiani and I. G. Murusidze, Phys. Scr. **45**, 87 (1992).
[20]E. Esarey, B. A. Shadwick, C. B. Schroeder, and W. P. Leemans, AIP Conf. Proc. **737**, 578 (2004).